Received: 14 December 2022 | Revised: 2 January 2023 | Accepted: 11 January 2023

DOI: 10.1002/pol.20220740

RESEARCH ARTICLE

JOURNAL OF POLYMER SCIENCE WILEY

Preparation of oriented poly(lactic acid) thin films by a combination of high temperature rubbing and thermal annealing: Impact of annealing parameters on structure, polymorphism and morphology

Marion Brosset[1,2] | **Laurent Herrmann**[1] | **Thierry Falher**[2] | **Martin Brinkmann**[1]

[1]Université de Strasbourg, CNRS, Strasbourg, France

[2]Centre Technique de la Plasturgie et des Composites, Pôle universitaire d'Alençon, Campus de Damigny, Damigny, France

Correspondence
Martin Brinkmann, Université de Strasbourg, CNRS, ICS UPR 22, F-67000 Strasbourg, France.
Email: martin.brinkmann@ics-cnrs.unistra.fr

Funding information
ANRT, Grant/Award Number: 2018/0723

Abstract

High temperature rubbing is a fast and low-cost method to prepare highly oriented films of polymers. This contribution describes the fabrication of smooth and pin-hole-free poly(lactic acid) (PLA) thin films of controlled structure and morphology using a combination of rubbing at moderate temperature ($T \leq 100°C$) and thermal annealing. We investigate the impact of annealing temperature and duration on the structure of rubbed PLLA and stereocomplex (SC) thin films. The importance of annealing parameters on polymorphism, crystallinity, crystal dimensions and in-plane orientation are analyzed using Transmission Electron Microscopy, Differential Scanning Calorimetry and FTIR spectroscopy. Regarding SC PLA films, the conditions are identified to fully transform the equimolar PLLA-PDLA blend films into pure oriented SC films without presence of homocrystals.

KEYWORDS

bio-sourced polymer, crystallization, poly(lactic acid), polymer films, structure

1 | INTRODUCTION

Poly(lactic acid) (PLA) is considered as a major commodity bio-sourced polymer of high interest for numerous applications such as packaging and medical use.[1–3] In addition, PLA is also biodegradable and is therefore considered as an alternative polymer for packaging to replace conventional fuel-based polymers.[4,5] The physical and mechanical properties of PLA depend strongly on the polymorphism, crystallinity and morphology that are determined by the processing/crystallization conditions.[6] As most semi-crystalline polymers, PLA has a typical polymorphism. PLLA can form at least four polymorphs: (i) the stable α form made of 10_3 helices organized in an orthorhombic unit cell, (ii) the pseudo-hexagonal α' structure that is a disordered form of the α structure, (iii) the β form made of 3_1 helices obtained under strong shear conditions and (iv) the γ form (10_3 helices) grown by epitaxy.[7,8] It has also been reported that PLLA can form a mesophase under tensile deformation of amorphous films at temperatures around 70°C.[9,10] Moreover, due to the presence of an asymmetric carbon in the chain of PLA, two enantiomers of PLA can

This is an open access article under the terms of the Creative Commons Attribution-NonCommercial-NoDerivs License, which permits use and distribution in any medium, provided the original work is properly cited, the use is non-commercial and no modifications or adaptations are made.
© 2023 The Authors. *Journal of Polymer Science* published by Wiley Periodicals LLC.

26424169, 0, Downloaded from https://onlinelibrary.wiley.com/doi/10.1002/pol.20220740 by Cochrane France, Wiley Online Library on [10/03/2023]. See the Terms and Conditions (https://onlinelibrary.wiley.com/terms-and-conditions) on Wiley Online Library for rules of use; OA articles are governed by the applicable Creative Commons License

be formed: poly(L-lactide) (PLLA) and poly(D-lactide) (PDLA). Equimolar blends of PLLA and PDLA form a stereocomplex (SC PLA) that can crystallize in a trigonal structure with a high melting temperature in the 220–230°C range.[11–14]

Different processing methods, such as alignment by hot drawing, biaxial drawing, epitaxy or addition of organic/inorganic nucleating agents can be used to control the PLA film structure and physical properties.[15–19] Nucleating agents such as clay, talc or small self-assembling molecules such as N-N′-N″-tricyclohexyl-1,-3,5-benzene-tricarboxylamide (TMAC) help monitor crystallinity in PLA.[19,20] Bai et al. showed that the nucleating agent tetramethylenedicarboxylic dibenzoyl-hydrazide self-assembles and form long fibrils that nucleate effectively PLA and thus help improve its barrier properties.[19] Such additives may have negative impacts, especially in the case of food packaging as they can migrate out of the polymer films and into food or other environments. Other methods that avoid the use of nucleating agents may therefore be relevant.

In this contribution, we focus on the preparation of oriented PLA thin films of thickness below 200 nm. Such oriented polymer films can be used as substrates for the oriented growth of a wide variety of small molecules and polymers.[21,22] Yan and coworkers used the melt-drawing method of Peterman to produce PLLA films only a few tens of nm thick with remarkable in-plane orientation.[23,24] Rubbed polymer surfaces of e.g. polyimides have been widely used as alignment layers for liquid crystals. Aligned thin films of poly(vinylidene-co-trifluoroethylene) can be used to enhance charge transport properties in non-volatile memories.[25] Melt-drawn PE substrates can be used to align molecular semi-conductors to achieve high field effect mobilities in OFETs.[26,27] Friction transfer of poly(tetrafluoroethylene) (PTFE) thin films is a method of choice since the oriented PTFE films show remarkable in-plane orientation and crystallinity, and are highly active nucleating surfaces for numerous molecular and macromolecular systems.[28,29]

In this contribution, we investigate the possibility to use surface rubbing to prepare highly oriented and crystalline PLA films. Recently, we have shown that high-T rubbing is an effective method to produce thin 15–150 nm-thick PLA films with a controlled in-plane orientation and polymorphism.[30] In this method, a rotating cylinder covered with a microfiber cloth is applied onto a thin film of PLA maintained at elevated and controlled rubbing temperature (T_R) to induce both chain alignment and crystallization of oriented PLA lamellae.[31–34] The choice of the rubbing temperature of PLA films determines the structure of the films: (i) oriented mesophase for $T_R = 80°C$, (ii) mixture of α and α' forms for $90°C \leq T_R \leq 140°C$ and (iii) pure α form for $T_R > 140°C$. In addition, highly oriented and pure films of the crystalline stereo-complex SC-PLA (i.e. with no PLLA or PDLA homo-crystals) were produced by high-T rubbing at 200°C of equimolar PLLA/PDLA blends. However, the rubbed PLA films produced at temperatures >140°C showed surface defects such as scratches and pinholes that are detrimental for applications such as gas barriers or for their use as gate dielectric and alignment layers of organic semiconductors in OFETs.

With the aim to overcome these limitations, we investigated the possibility to combine a rubbing at lower temperature in the range 80–100°C that preserves the smooth film morphology with a thermal annealing step. We identify the optimal parameters (annealing time T_A and duration t_A) for the preparation of highly oriented and crystalline PLLA and pure stereo-complex (SC) thin films. The impact of annealing parameters on polymorphism, crystallinity and film morphology were established by a combination of POM, TEM, FTIR spectroscopy and DSC.

2 | EXPERIMENTAL SECTION

2.1 | Materials

Pure Poly(L-lactide) (reference Luminy L175) and Poly(D-lactide) (reference Luminy D120) were purchased from Total Corbion. The macromolecular parameters obtained by Size Exclusion Chromatography (SEC) of PLLA polymer samples used in this study are given in reference 30. Sodium Poly(styrenesulfonate) (NaPSS) was purchased from Sigma Aldrich.

2.2 | Thin films preparation and orientation

The preparation of oriented poly(lactic-acid) films by high-temperature mechanical rubbing follows the procedure described in reference 30. To perform TEM studies, PLA is deposited on a sacrificial layer of NaPSS on glass slides. NaPSS films are spin-coated on clean glass slides using a 10 mg/ml aqueous solution (3000 rpm for 60 s). Glass substrates are cleaned by ultrasonication for 15 min successively in acetone, ethanol, aqueous solution of Hellmanex and rinsed three times in distilled water. Thicker PLA films are doctor-bladed on NaPSS/glass using a 10 mg/ml solution in chloroform at 50°C. The film thickness was measured by ellipsometry (see Figure S1 in ref. 30). Prior to rubbing, the PLLA films are melted at 190°C for 1 min and quenched in ice water to obtain glassy (amorphous) PLLA films that are suitable for alignment by rubbing.

26424169, 0, Downloaded from https://onlinelibrary.wiley.com/doi/10.1002/pol.20220740 by Cochrane France, Wiley Online Library on [10/03/2023]. See the Terms and Conditions (https://onlinelibrary.wiley.com/terms-and-conditions) on Wiley Online Library for rules of use; OA articles are governed by the applicable Creative Commons License

For the alignment of the PLA films, a homemade rubbing machine is used as described in our previous publications.[31–34] A rotating cylinder (600 RPM) covered with a microfiber cloth is applied with a pressure of ca. 2–3 bar on a translating sample holder (1 cm/s). Before rubbing, the sample is allowed to equilibrate for 30 s on the sample holder heated at T_R, the rubbing temperature.

2.3 | Structural analysis, differential scanning calorimetry and FTIR spectroscopy

For TEM measurements, PLA films are coated with a thin 2 nm-thick amorphous carbon film and removed from the glass substrate by floating on distilled water. Films are subsequently recovered on TEM copper grids. A CM12 TEM was used in low dose bright field and diffraction modes. It is equipped with a MVIII camera (Soft Imaging System). To observe the lamellar structure in bright field TEM with sufficient contrast, thin films of 50 nm thickness were prepared from 5 mg/ml PLLA solution. Calibration of the Diffraction (ED) patterns was made with an oriented poly(tetrafluoroethylene) (PTFE) thin film prepared by friction transfer.

Differential Scanning Calorimetry (DSC) experiments were performed on a TA Instruments DSC Q200. Three mg of oriented PLA films (8–10 rubbed films) were recovered by floating on distilled water and collected in an aluminum DSC pan. One heating and one cooling steps in a temperature range 40–210°C were used to characterize the films after alignment by rubbing (10°C/min). The DSC scans shown in the following correspond to the first heating.

Fourier Transform Infra-Red (FTIR) spectroscopy was performed using a Perkin Elmer Spectrum Two spectrophotometer in transmission mode. The PLA samples were transferred by floating on distilled water to Si(100) substrates (Silchem). The spectra were recorded in the 400–4000 cm^{-1} spectral range, with a resolution of 4 cm^{-1}. For each sample 16 scans were recorded to generate an average spectrum.

3 | RESULTS AND DISCUSSION

3.1 | Impact of annealing temperature on the crystal size and crystallinity of rubbed PLLA films

To limit and suppress the formation of micro-scratches produced when PLLA films are rubbed at high temperature (>140°C), the experimental process was split in two steps. First, the solution-cast, un-oriented PLA film is rubbed at a lower temperature (in the range 80–100°C) in order to pre-align the films. Second, the PLA films are subjected to one thermal annealing at a higher temperature designed to further crystallize the films. Thermal annealing of a pre-aligned film by rubbing affects several features of the film structure such as crystal polymorphism, mosaicity of PLA crystalline domains (distribution of in-plane orientation and contact planes), crystallinity and crystal dimensions. For PLLA, the two rubbing conditions resulted in different polymorphs. When $T_R = 80°C$ the oriented PLA is an aligned mesophase. When $T_R = 100°C$ the films are a mixture of oriented α/α'forms.[26] In both cases, the films are very smooth (see Figure S1), contrary to films rubbed at $T_R = 140°C$ that present pinholes and scratches (see Figure for the title of content). The thermal annealing conditions (temperature T_A and time t_A) were evaluated to reach the highest crystallinity while maintaining high in-plane orientation of the rubbed PLLA films. The last item deals with the impact of the initial film structure (oriented mesophase versus α/α'mixture) on the annealed film structure as a function of annealing conditions.

TEM in Bright Field and diffraction modes were used to characterize the structure and in-plane orientation versus annealing conditions for 50-150 nm-thick films. Figure 1(A) shows the evolution of the electron diffraction patterns of PLLA films rubbed at 100°C and subsequently annealed at temperatures in the range 145–170°C for 5 min. The section profiles in Figure 1(B) show the evolution of the equatorial reflections versus annealing temperature T_A.

For $T_R = 100°C$, the as-rubbed PLLA films show only a few reflections (mainly 2 0 0 and 2 0 3) characteristic of the disordered α' form crystals of PLLA with a preferential (010) contact plane on the substrate (presumably imposed by the rubbing). After annealing at increasing T_A, more and more new reflections appear. They are both better defined and sharper, as expected for a film recrystallization. Reflections become also sharper when T_A reaches 165°C, and thus approaches the T_m of PLLA (≈175°C). Among them, the 1 0 3 and 1 0 7 reflections of the α form indicate that the α' crystals of the rubbed PLLA films transform to α form upon annealing. This diffraction evidence is consistent with the DSC and FTIR results (Figure 3 and S2). For $T_A = 170°C$, partial melting results in an irreversible loss of in-plane orientation as indicated by the very broad arced reflections (especially for the 2 0 0). Accordingly, $T_A = 165°C$ is the optimal annealing temperature to obtain fully aligned and crystalline α form PLLA.

Thermal annealing not only impacts the crystallinity of the films and the dimensions of the crystals, it has also

26424169, 0, Downloaded from https://onlinelibrary.wiley.com/doi/10.1002/pol.20220740 by Cochrane France, Wiley Online Library on [10/03/2023]. See the Terms and Conditions (https://onlinelibrary.wiley.com/terms-and-conditions) on Wiley Online Library for rules of use; OA articles are governed by the applicable Creative Commons License

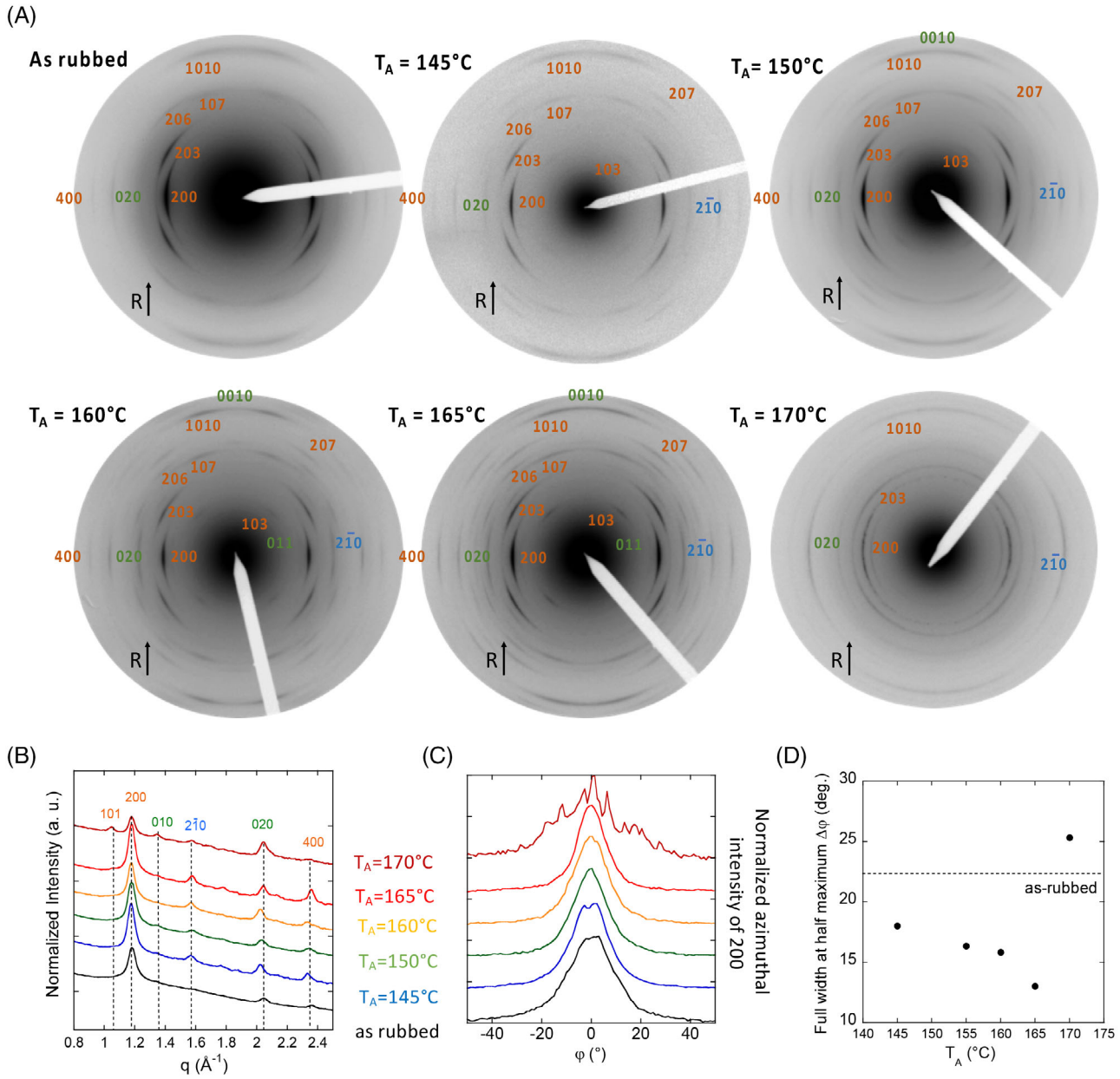


FIGURE 1 (A) Electron diffraction patterns of rubbed PLLA films ($T_R = 100°C$) as a function of the annealing temperature (T_A) in the range 140–170°C. The annealing time was fixed at 5 min. The rubbing direction is vertical. Main reflections are indexed (α form). Indices noted in orange, green and blue correspond to the contact planes (010), (100) and (120) respectively. (B) Equatorial section profiles of the ED patterns of rubbed PLLA films as a function of the annealing temperature T_A. (C) Evolution of the section profile showing the azimuthal in-plane intensity distribution of the 2 0 0 reflections versus annealing temperature. For clarity, the section profiles were normalized in intensity and shifted along the ordinate axis. (D) Full width at half maximum of the 2 0 0 reflection versus annealing temperature T_A.

an important impact on the in-plane and out-of-plane distributions (mosaicity) of the PLA crystal orientations. The mosaicity relates to both (i) the distribution of crystal contact planes and to (ii) the in-plane orientation distribution of chain directions. In Figure 1(B) the increasing number of *hk0* equatorial reflections with T_A is not only related to a higher crystal perfection, it also points at new contact planes such as (100) and (120) of PLLA crystals when $T_A \geq 145°C$. The presence of new contact planes suggests that the recrystallization of the rubbed films leads to a kind of fiber-structure of the films, with the fiber axis corresponding to the rubbing direction.

The mosaicity is also characterized by the distribution of in-plane chain orientations. The latter can be quantified by the azimuthal in-plane profile of the 2 0 0 reflection and thus followed versus T_A (Figure 1C).

26424169, 0, Downloaded from https://onlinelibrary.wiley.com/doi/10.1002/pol.20220740 by Cochrane France, Wiley Online Library on [10/03/2023]. See the Terms and Conditions (https://onlinelibrary.wiley.com/terms-and-conditions) on Wiley Online Library for rules of use; OA articles are governed by the applicable Creative Commons License

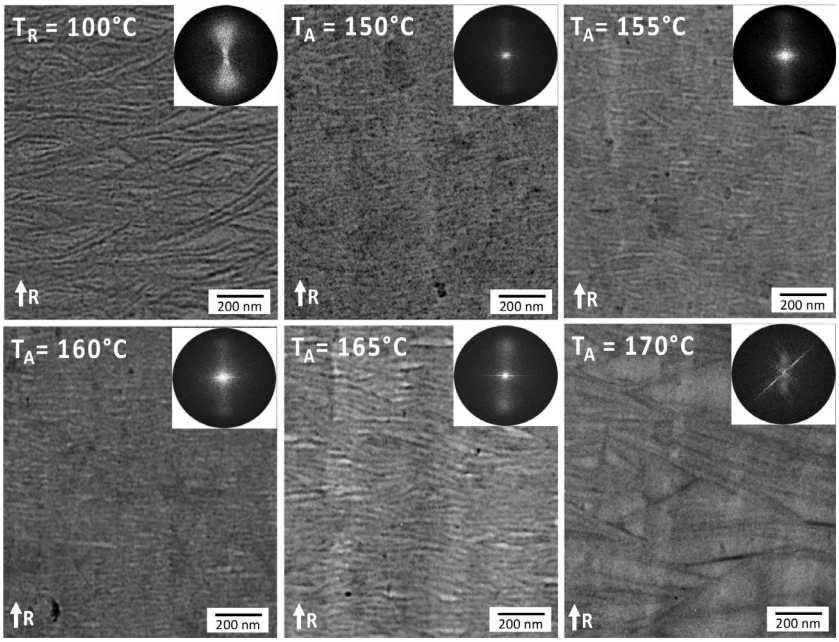


FIGURE 2 Evolution of the lamellar morphology in rubbed PLLA films ($T_R = 100°C$) as a function of the annealing temperature T_A (the annealing time was 5 min). The insets show the FFT of the BF images. The rubbing direction is vertical.

With increasing T_A, a progressive narrowing of the 2 0 0 peak in-plane distribution is observed up to 165°C. As seen in Figure 1(D), the FWHM of the 2 0 0 decreases from 18° for as-rubbed films ($T_R = 100°C$) to 13° for a film annealed in a further step at $T_A = 165°C$. For $T_A = 170°C$ on the contrary, the FWHM increases to 26°: melting of the film results in a partial loss of in-plane orientation. Before the melting step however, the thermal annealing not only promotes the α'→ α melt-recrystallization, but the α form crystals display enhanced in-plane orientation. This is in contrast to the mosaicity of the α crystals associated to their contact plane distribution that broadens upon annealing.

To investigate the impact of thermal annealing on the film morphology, bright Field TEM was used. This approach is particularly valuable for such oriented films since the lamellae organization, seen edge-on, is highlighted. Bright field images of oriented PLLA films rubbed at 100°C and subsequently annealed at different temperatures in the range 150–165°C are displayed in Figure 2. When only rubbed at 100°C the films already are made of well-defined lamellae but their density is low. This loose packing is also documented by the lack of clear lamellar periodicity in the Fast Fourier Transform (FFT) of the BF (insets in Figure 2). The situation changes after thermal annealing. For $T_R \geq 150°C$, a tight packing of edge-on oriented PLLA lamellae is observed. The lamellar periodicity increases also progressively: from 24 nm at $T_A = 150°C$ to more than 30 nm at 165°C. For $T_A = 170°C$, melting of the films results in a loss of in-plane orientation and only few edge-on PLLA lamellae remain visible.

To conclude, TEM demonstrates that, starting with films rubbed at 100°C, the subsequent annealing parameters $T_A = 165°C$ and $t_A = 5$ min are most adequate to produce highly in-plane oriented and crystalline α -form PLLA films. The added advantage of this two-steps procedure is to avoid the formation of scratches and pinholes as seen for PLLA films produced in a single rubbing step at 140°C.

3.2 | Impact of annealing time on the crystallinity of rubbed PLLA films

Figure 3 collects the first heating scans of PLLA films rubbed at 80°C and 100°C and for the same samples after thermal annealing. A broad exotherm centered around 85°C is observed for the films rubbed at 80°C. According to the literature on PLLA films stretched slightly above T_g, this exotherm indicates the transformation of the oriented PLLA mesophase into α' phase.[34,36] This exotherm is fully suppressed after thermal annealing for 1 min at 165°C: only the melting endotherm of crystalline α PLLA centered at 175°C is observed. The PLLA films rubbed at 100°C do not show any exotherm around 85°C since they are formed of the oriented α' phase. A small exotherm is present close to the melting. It corresponds to the melting of the α' phase and its recrystallization in the α phase that subsequently melts at higher temperature. Again, after thermal annealing, the films rubbed at 100°C shows only a single melting endotherm with no trace of the α' → α exotherm, indicating that all α' phase transformed to α phase during the annealing step.

26424169, 0, Downloaded from https://onlinelibrary.wiley.com/doi/10.1002/pol.20220740 by Cochrane France, Wiley Online Library on [10/03/2023]. See the Terms and Conditions (https://onlinelibrary.wiley.com/terms-and-conditions) on Wiley Online Library for rules of use; OA articles are governed by the applicable Creative Commons License

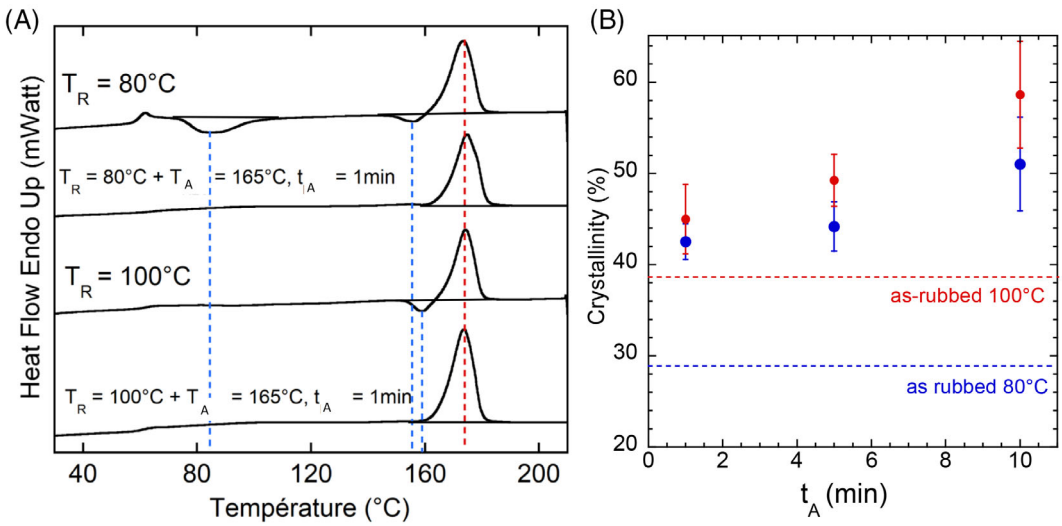


FIGURE 3 (A) DSC traces of the first annealing scan of PLLA thin films rubbed at 80 and 100°C. Cold crystallization exotherms are highlighted in blue whereas melting endotherms are shown in red. Evolution of the crystallinity (B) extracted from the melting enthalpies for PLLA films rubbed at 80°C (blue) and 100°C (red) and annealed at 165°C for different times.

DSC was also used to identify the most appropriate thermal annealing time t_A to produce highly crystalline PLLA films. Figure 3(B) displays the crystallinity reached (as determined from the melting enthalpy) as a function of the annealing time t_A at 165°C. The increases are substantial. For the films rubbed at $T_R = 80$°C with, admittedly a < 30% initial crystallinity, this value nearly doubles after 10 min annealing. Films rubbed at 100°C have higher initial crystallinities, but the relative improvements are less, but the final values reached are significant and always higher than for the 80°C rubbed films. The 58% ± 5% levels reached compare well with corresponding values reported in the literature (cf. Table 1). Li et al. indicate 55% for PLLA films oriented by the melt-drawing method of Petermann et al.[23,24] In both cases, the values are above those reported for PLLA films crystallized in the presence of nucleating agents (Poly(ethyleneglycol): 46%, talc: 40%, TMC-328: 51%). These encouraging results suggest that rubbing at a moderate temperature above T_g followed by annealing close to the melting temperature is an effective method to produce highly oriented and highly crystalline films of PLLA.

The above structural changes induced by thermal annealing were also followed and actually confirmed by FTIR spectroscopy.[40,41] Figure S2 shows the evolution of the FTIR spectra of PLLA films rubbed at 100°C after annealing at 165°C for 5 min. The α' → α transformation is clearly evidenced in the range 1200–1400 cm^{-1}, for the $\delta_{(CH)} + \delta_{s(CH3)}$ modes with a splitting of the peak around 1300 cm^{-1}. In the 800–1000 cm^{-1} range, the 871 cm^{-1} band corresponding to the $\nu_{(C\text{-}COO)}$ mode becomes sharper and more intense after annealing, indicating an increased crystallinity. The intensity of the 922 cm^{-1} band assigned to the $\nu_{(C\text{-}C)}$ mode increases after

TABLE 1 Different values of PLLA and SC-PLA crystallinity in rubbed and annealed thin films as compared to the literature

System	Crystallinity (%)	Reference
PLLA		
Rubbing at 145°C	53 ± 2	30
Rubbing 100°C + thermal annealing (5 min) at 165°C	58 ± 5	This work
Melt-drawing	55	23
Nucleating agents		
Talc	40	36
PEG	46	35
TMC-328*	51	19
SC-PLA		
$T_R = 100$°C + annealing 200°C (5 min)	35	This work
PDLA/PLLA blend with additive EMA-GMA**	36.5	36
Co-extrusion at 200°C	59	37
Melt spinning at high speed	37	38
Templating using residual SC-PLA crystals	47	39

*TMC-328: N,N′,N″-tricyclohexyl-1,3,5-benzenetricarboxylamide.
**EMA-GMA: poly(ethylene-ran-methacrylate-ran-glycidyl methacrylate).

26424169, 0, Downloaded from https://onlinelibrary.wiley.com/doi/10.1002/pol.20220740 by Cochrane France, Wiley Online Library on [10/03/2023]. See the Terms and Conditions (https://onlinelibrary.wiley.com/terms-and-conditions) on Wiley Online Library for rules of use; OA articles are governed by the applicable Creative Commons License

annealing. It corresponds to the formation of the more ordered α form and the corresponding disappearance of the original α' form.

3.3 | Impact of annealing duration and initial structure of rubbed PLLA films

Depending on the rubbing temperature, the PLLA films show different initial structures prior to thermal annealing. When $T_R = 80°C$, the films are an oriented mesophase; when $T_R = 100°C$, they are a mixture of aligned α/α' forms. The impact of the annealing *duration* at 165°C was thus analyzed for these two rubbing temperatures – in fact, for these two different initial crystal structures.

Figures 4(A) and (B) display the diffraction patterns for $T_R = 80°C$ and 100°C, respectively. In Figure 4(C, D) present equatorial section profiles of the ED patterns versus annealing time t_A for $T_R = 80°C$ and 100°C. Figure S3 shows the section profiles of the ED pattern along the vertical layer line corresponding to h = 2. For $T_R = 80°C$, the as-rubbed PLLA film display a very limited set of reflections, essentially 2 0 0 and 2 0 3. After even short (1 min) annealing times at 165°C many new reflections of the α form are observed for the films rubbed at 80°C and 100°C, indicating significant levels of recrystallization, in agreement with DSC and FTIR results.

The impact of annealing time t_A on the PLLA films structure is also illustrated by the evolution the reflections on meridional layer line with h = 2. In Figure S3, their vertical section profiles are plotted as a function of t_A for films rubbed at 100°C and annealed at 165°C. For $t_A \geq 1$ min, new mixed index reflections appear, that are of the α form of PLLA (e.g. 2 0 6 and 2 0 7). Their intensity increases for annealing times $t_A \geq 5$ min, in agreement with the global crystallinity increase determined by DSC. In the present case however, the observed variations may also indicate structural rearrangements, namely out-of-plane reorientation of crystallites induced by the development of additional contact planes. In other words, these ED patterns are typical of oriented *fibers* with the fiber axis determined by the rubbing direction. The fully aligned α crystals after annealing at 165° indicate that both the mesophase and the α' crystals formed by rubbing at 80°C and 100°C acted as seeds for the oriented growth of the stable α phase. Overall, annealing times t_A in the 5–10 min range are best suited for the preparation of highly oriented and crystalline PLLA films since crystal transformation is completed.

Minor differences between films rubbed at 80°C and 100°C and annealed do however exist, that may be worth mentioning. Their in-plane orientation and structure are quite similar. However, both lower peak intensities and broader angular dispersion (in particular of the 2 0 0 reflection) for the films rubbed at 80°C indicate lower levels of crystallinity (in agreement with the DSC results) and crystal orientation. Even after thermal annealing the initial structure of pre-aligned PLLA films (oriented mesophase versus α' form) influences the final levels of crystal perfection that can be reached.

3.4 | Preparation of oriented SC PLA thin films

As reported previously, rubbing equimolar blends of PLLA/PDLA at a high temperature (200°C) produces "pure" oriented SC PLA films, without any homocrystals.[30] However, the surface morphology is severely damaged by rubbing at such elevated temperatures. To overcome this weakness, and as for PLLA, we investigated the possibility to prepare pure oriented SC-PLA films by resorting to a combination of low-T rubbing and thermal annealing.

3.4.1 | Impact of the annealing temperature on the structure of PLLA/PDLA equimolar blends

Figure 5(A) illustrates the evolution of the diffraction pattern of a rubbed PLLA/PDLA blend film (1:1) as a function of the annealing temperature T_A (annealing time of 5 min, quenching to RT). Annealing was performed directly on the PLA film deposited on the TEM grid. The as-rubbed blend film shows the typical ED pattern of oriented PLLA and PDLA homo-crystals, with its typical 2 0 0 and 2 0 3 reflections. At 160°C, i.e. below the full melting of the homo-crystals, the ED has already changed to a composite pattern with overlapping contributions of the oriented homo-crystals α form and oriented SC-PLA. At this stage, the SC-PLA reflections are rather fuzzy and of low intensity. As soon as T_A exceeds the melting temperature of homo-crystals T_m^{hc}, the 2 0 0 reflection of PLLA and PDLA homo-crystals disappear, leaving only the characteristic SC-PLA reflections (see section profile in Figure 5B). All PLLA/PDLA homo-crystals (hc) melted and recrystallized to form oriented SC-PLA for $T_A > T_m^{hc}$. Importantly, this melt-recrystallization does not disturb the in-plane alignment. It turns out that seeds of oriented SC-PLA are already present in the blend films rubbed at 100°C, as assessed by the presence of a very weak 3 0 0 peak of the SC-PLA in the ED for $T_R = 100°C$. Oriented SC-PLA seeds can indeed be formed at low T_R and induce alignment in the melt-recrystallized blend

26424169, 0, Downloaded from https://onlinelibrary.wiley.com/doi/10.1002/pol.20220740 by Cochrane France, Wiley Online Library on [10/03/2023]. See the Terms and Conditions (https://onlinelibrary.wiley.com/terms-and-conditions) on Wiley Online Library for rules of use; OA articles are governed by the applicable Creative Commons License

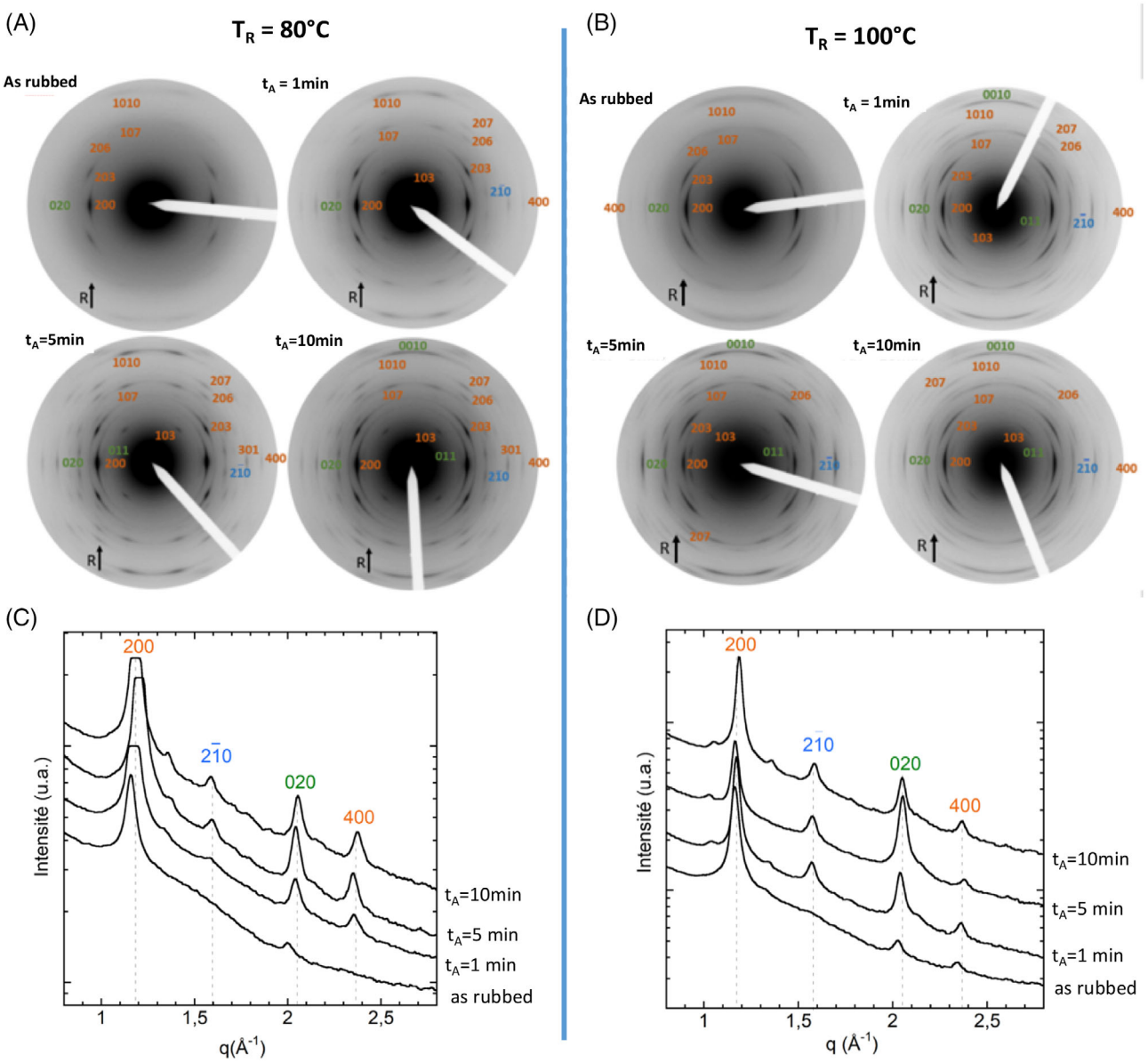


FIGURE 4 Diffraction patterns of PLLA films rubbed at 80°C (A) and 100°C (B) and subsequently annealed at 165°C during different times in the range 1 – 10 min. The rubbing direction *R* is vertical. The most intense reflections were indexed (α form). Indices in orange, green and blue correspond to (010), (100) and (120) contact planes respectively. The lower part of the figure shows the equatorial section profiles of the ED patterns as a function of the annealing time t_A for $T_R = 80°C$ (C) and for $T_R = 100°C$ (D). For clarity, the profiles were shifted along the ordinate axis. Note in (C) that the 200 peak is saturated in intensity for the annealed films.

films of PLLA/PDLA (see schematic illustration in Figure 5D). The situation reminds the case of bisphenol A polycarbonate (PC) films rubbed in their amorphous phase at room temperature that can be fully crystallized in the form of oriented lamellae when subjected to vapor phase annealing [42]. Rubbing at RT i.e. far from the crystallization temperature of PC was sufficient to observe the formation of aligned seeds by Atomic Force Microscopy. The surface density of oriented seeds was directly related to the so-called rubbing length, a larger rubbing length leading to a higher density of seeds. Clearly, rubbing triggers the formation of oriented SC-PLA seeds in equimolar PLLA/PDLA blend films that help further crystallize the stereo-complex upon subsequent thermal annealing. Possibly, the shear force during rubbing is sufficient to create elongated stems of oriented PLLA and PDLA chains that can thus form more readily SC-PLA seeds by preferential inter-chain interactions. When T_A reaches 190°C, a pure oriented SC-PLA film is obtained. The progressive improvement of crystallinity and crystal

26424169, 0, Downloaded from https://onlinelibrary.wiley.com/doi/10.1002/pol.20220740 by Cochrane France, Wiley Online Library on [10/03/2023]. See the Terms and Conditions (https://onlinelibrary.wiley.com/terms-and-conditions) on Wiley Online Library for rules of use; OA articles are governed by the applicable Creative Commons License

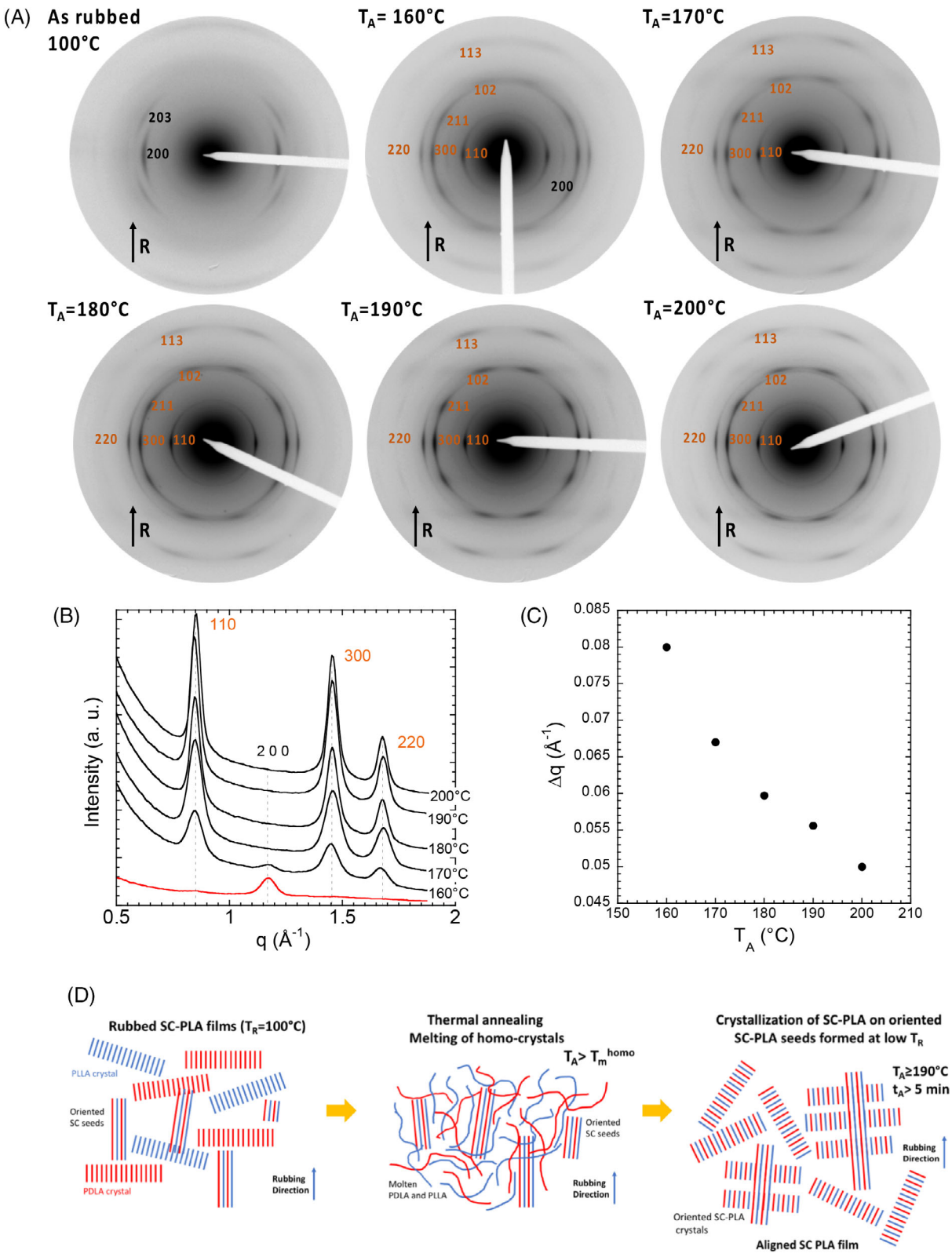


FIGURE 5 (A) Evolution of the ED patterns of rubbed PLLA/PDLA equimolar blend films ($T_R = 100°C$) as a function of the annealing temperature T_A (duration of annealing of 5 min). The rubbing direction is vertical. The indices for the reflections of the PLLA and PDLA homo-crystals are in black whereas the reflections of the SC-PLA phase are noted in orange. (B) Equatorial section profiles of the ED patterns versus annealing temperature (T_A). (C) FWHM of the 3 0 0 reflection of SC-PLA versus annealing temperature T_A. (D) Schematic illustration of the growth of oriented SC-PLA films by a combination of rubbing at 100°C and thermal annealing at 190–200°C based on the presence of oriented SC-PLA seeds generated by high-T rubbing.

26424169, 0, Downloaded from https://onlinelibrary.wiley.com/doi/10.1002/pol.20220740 by Cochrane France, Wiley Online Library on [10/03/2023]. See the Terms and Conditions (https://onlinelibrary.wiley.com/terms-and-conditions) on Wiley Online Library for rules of use; OA articles are governed by the applicable Creative Commons License

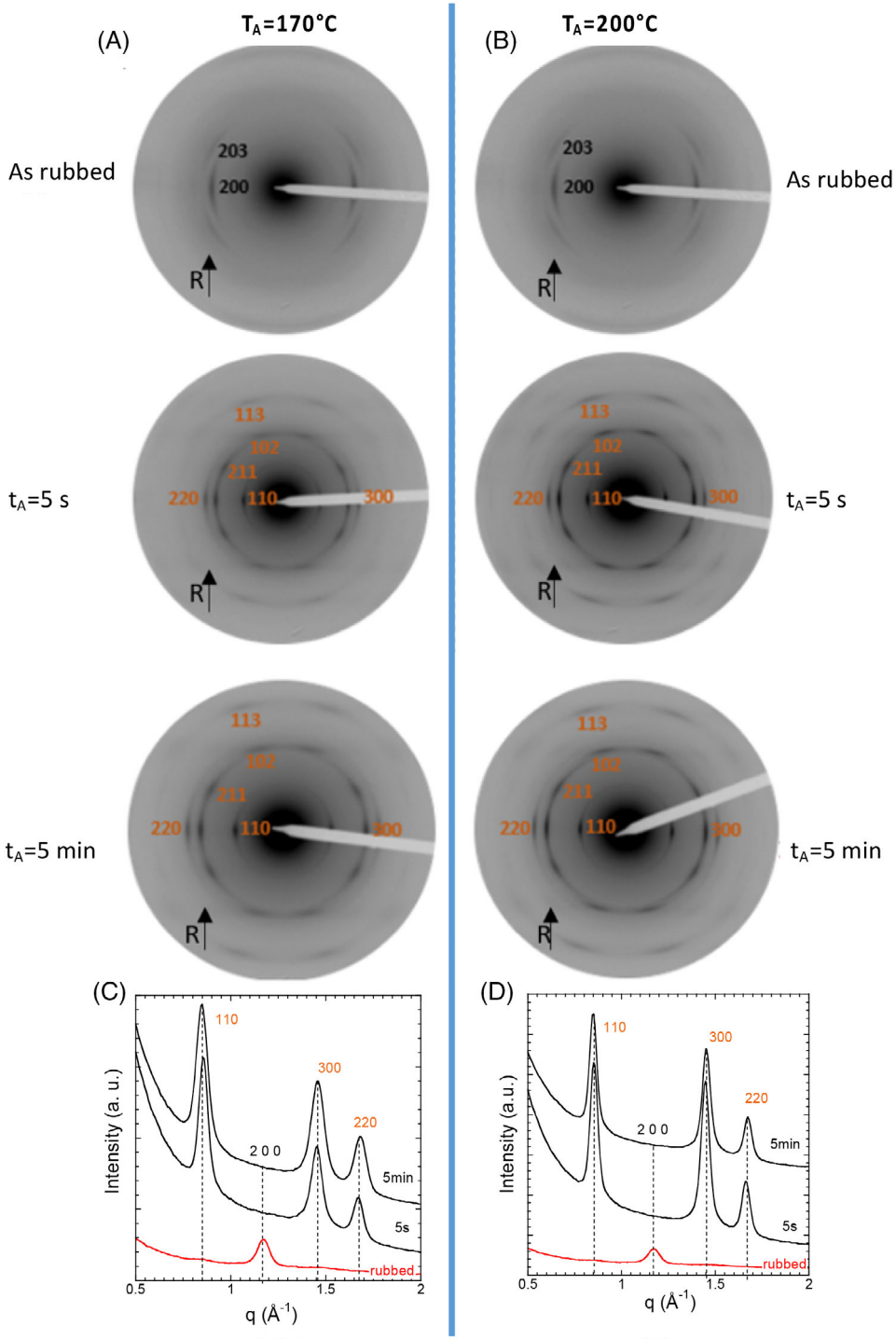


FIGURE 6 Impact of annealing time (t_A) on the electron diffraction patterns of rubbed PLLA/PDLA equimolar blend films ($T_R = 100°C$, 50 nm). The rubbing direction is vertical. The indices for the reflections of the PLLA and PDLA homocrystals are in black whereas the reflections of the SC-PLA phase are noted in orange. Equatorial section profiles of the ED patterns versus annealing time for $T_A = 170°C$ (B) and $T_A = 200°C$ (C).

size domains and increase in size can be followed through the FWHM of the 3 0 0 reflection versus T_A (Figure 5C). Annealing at a higher T_A of 200°C does not further improve the film structure. The increased arcing of the ED reflection suggests even a possible loss of in-plane orientation when T_A approaches T_m^{SC} (The FWHM of the 2 0 0 reflection Δq reduces from 0.08 Å^{-1} at $T_A = 160°C$ to less than 0.05 Å^{-1} for $T_A = 200°C$). Given these opposite trends the choice of T_A can only be a compromise between optimal crystallinity that requires T_A close to T_m^{SC} and high in-plane orientation of SC crystals that is better preserved at lower T_A.

3.4.2 | Impact of the annealing time on the structure of PLLA/PDLA equimolar blends

Figure 6 illustrates the evolution of the structure in oriented blend films PLLA/PDLA obtained by rubbing at

26424169, 0, Downloaded from https://onlinelibrary.wiley.com/doi/10.1002/pol.20220740 by Cochrane France, Wiley Online Library on [10/03/2023]. See the Terms and Conditions (https://onlinelibrary.wiley.com/terms-and-conditions) on Wiley Online Library for rules of use; OA articles are governed by the applicable Creative Commons License

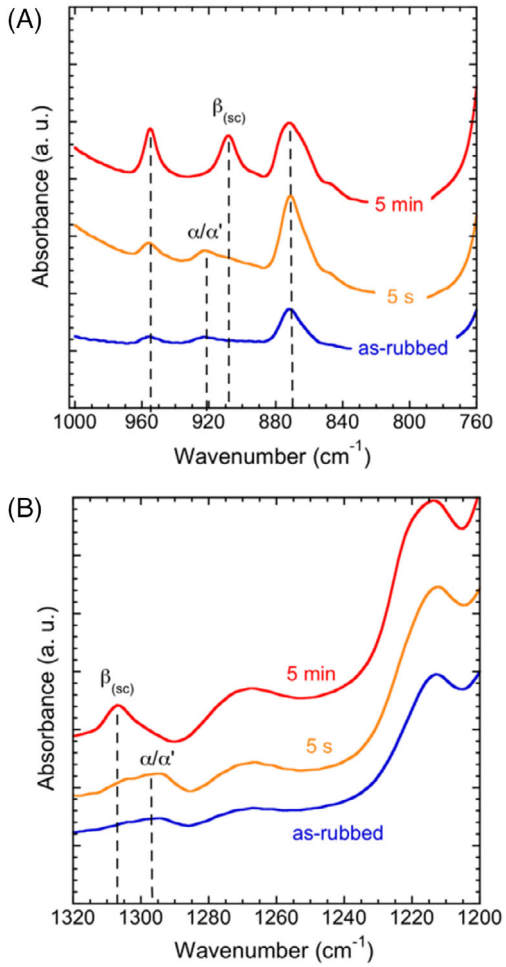


FIGURE 7 Evolution of the FTIR spectra of rubbed PLLA/PDLA (1:1) blend films rubbed at $T_R = 100°C$ as function of the annealing time t_A at $T_A = 200°C$. (A) 800–1000 cm^{-1} range and (B) 1200–1320 cm^{-1}. For clarity, spectra were shifted along the ordinate axis.

$T_R = 100°C$ as a function of the annealing time t_A for $T_A = 170°C$ and $T_A = 200°C$. Annealing at a temperature slightly above T_m^{homo} for even a very short time (5 s) is sufficient to transform the original α'/α form in the oriented SC-PLA. According to these ED results, no major improvement can be recorded for longer annealing times, except for a minor increase of the 3 0 0 reflections. It turns out however that, for this specific investigation, IR and DSC analyses are more pertinent.

The transformation kinetics of the rubbed blend films into SC-PLA as observed by FTIR spectroscopy are illustrated in Figure 7. The films are made of equimolar PLLA/PDLA, are rubbed at 100°C and annealed at 200°C. The different chain conformations of the homo-crystal phases α, α' and the stereocomplex phase have specific IR signatures. The bands centered at 924 cm^{-1} and 1296 cm^{-1} indicate the 10_3 chain conformation of the α/α' homocrystals, the 908 cm^{-1} and 1306 cm^{-1} bands correspond to the 3_1-chain conformation of the SC-PLA. As seen in Figure 7, and quite expectedly, annealing for 5 s at 200°C reduces the intensity of the α/α' IR bands as new bands that correspond to SC-PLA appear. After $t_A = 5$ s therefore SC-PLA and homo-crystals still coexist. It is only after a longer annealing time ($t_A = 5$ min) that the IR bands of PLLA/PDLA homo-crystals nearly vanish and are replaced by the bands of the SC-PLA. These results are in line with a DSC analysis of the rubbed PLLA/PDLA blend films. DSC shows indeed that a 5 min annealing at 200°C is necessary to reduce the remaining melting enthalpy ΔH_m of the homocrystals to less than 10% of the original value in the as-rubbed films (see Figure S4). Accordingly, the kinetics of the process of full crystallization of the blend films in crystalline oriented SC-PLA is better captured by global investigation techniques - DSC and FTIR spectroscopy, which in addition help evaluate the final crystallinities reached. In this case, electron diffraction may be too local a probe. From Figure 6, it remains that the T_A, when in the 170°C-200°C range, has little influence on the time necessary to fully convert the blend films into crystalline and oriented SC-PLA.

4 | CONCLUSION

Oriented and crystalline thin films of PLLA and SC-PLA have been prepared by combining rubbing at a moderate temperature in the 80–100°C range and a thermal annealing step to preserve to the extent possible the smooth surface of the PLA films. The optimal rubbing T_R and annealing temperatures T_A and time t_A have been determined for both PLLA and the stereocomplex of PLLA and PDLA. The resulting structures and morphologies of the films were studied by TEM. For PLLA, oriented films with a very high crystallinity (up to 58%) are obtained when $T_R = 100°C$, $T_A = 165°C$ and $t_A = 5$ min. With the PLLA/PDLA blends, almost pure crystalline SC-PLA for $T_R = 100°C$, $T_A = 200°$ for 5 min. These optimal annealing conditions will be used in a forthcoming study to prepare 20 μm-thick aligned PLLA films. It appears that the production of oriented polymer films by high-temperature rubbing followed by thermal annealing is appealing to a large palette of polymers. First among them polymers with high melting temperatures needing rubbing close to their melting temperatures. Numerous conjugated polymers that have melting temperatures beyond 300°C are potential candidates. Of interest are some donor-acceptor low bandgap polymers such as poly(benzodithiophene-alt-dithienyl difluorobenzotriazole) used for instance in polarized photodetectors.[43]

A simple and versatile method combining rubbing and annealing can be used to fabricate smooth polymer

26424169, 0, Downloaded from https://onlinelibrary.wiley.com/doi/10.1002/pol.20220740 by Cochrane France, Wiley Online Library on [10/03/2023]. See the Terms and Conditions (https://onlinelibrary.wiley.com/terms-and-conditions) on Wiley Online Library for rules of use; OA articles are governed by the applicable Creative Commons License

films with controlled orientation and crystal dimensions. In the present study, it has been used to prepare PLA films with controlled surface texture. In a wider context, such films could be useful as alignment layers and direct the growth of H-bonding molecules and/or polymers. For example, the oriented SC-PLA films prepared in this study would be suitable alignment layers for the oriented growth of molecular and macromolecular systems that require melt-crystallization up to 200°C. Such model surfaces may also help study epitaxial processes at play at the interface between PLLA and other polymers of interest such as poly(hydroxyalkanoate)s.

ACKNOWLEDGMENTS

We thank the TEM platform (M. Schmutz) from ICS for technical support. Support from ANRT through Cifre PhD grant 2018/0723 is acknowledged (MB). Céline Kiefer and Guillaume Rogez (IPCMS, Strasbourg) are acknowledged for giving access to the FTIR spectroscopy laboratory. Mélanie Legros is acknowledged for performing the GPC analysis of the PLLA materials. We thank also Catherine Saettel for the DSC measurements. We want also to thank Bernard Lotz for a critical reading of the manuscript and fruitful discussions on PLA polymorphism.

CONFLICT OF INTEREST

The authors declare no conflict of interest.

ORCID

Martin Brinkmann https://orcid.org/0000-0002-2680-1506

REFERENCES

[1] L.-T. Lim, R. Auras, M. Rubino, *Prog. Polym. Sci.* **2008**, *33*, 820.
[2] K. Matsunari, Y. Kimura, in *Synthesis, Structure and Properties of Poly(Lactic acid). Advances in Polymer Science* (Eds: M. di Lorenzo, R. Androsch), Springer, Cham **2017**.
[3] M. Vert, S. M. Li, G. Spenlehauer, P. Guerin, *J. Mater. Sci. Mater. Med.* **1992**, *3*, 432.
[4] R. M. Rasal, A. V. Janorkar, D. E. Hirt, *Prog. Polym. Sci.* **2010**, *35*, 338.
[5] M. Cocca, M. L. di Lorenzo, M. Malinconico, V. Frezza, *Euro. Polym. J.* **2011**, *47*, 1073.
[6] M. L. di Lorenzo, R. Androsch, *Polym. Int.* **2019**, *68*, 320.
[7] S. Saeidlou, M. A. Huneault, H. Li, C. B. Park, *Prog. Polym. Sci* **2012**, *37*, 1657.
[8] B. Lotz, in *Synthesis, Structure and Properties of Poly(Lactic acid). Advances in Polymer Science* (Eds: M. di Lorenzo, R. Androsch), Springer, Cham **2017**.
[9] G. Stoclet, R. Seguela, J. M. Lefebvre, S. Elkoun, C. Vanmansart, *Macromolecules* **2010**, *43*, 1488.
[10] Y. Wang, M. Li, K. Wang, C. Shao, Q. Li, C. Shen, *Soft Matter* **2014**, *10*, 1512.
[11] Y. Ikada, K. Jamshidi, H. Tsuji, S. H. Hyon, *Macromolecules* **1987**, *20*, 904.
[12] L. Cartier, T. Okihara, Y. Ikada, H. Tsuji, J. Puiggali, B. Lotz, *Polymer* **2000**, *41*, 8909.
[13] H. Tsuji, *Macromol. Biosci.* **2005**, *5*, 569.
[14] H. Bai, S. Deng, D. Bai, Q. Zhang, Q. Fu, *Macromol. Rapid Commun.* **2017**, *38*, 1700454.
[15] A. Guinault, G. H. Menary, C. Courgneau, D. Griffith, V. Ducruet, V. Miri, C. Sollogoub, *AIP Conf. Proc.* **2011**, *1353*, 826.
[16] G. Kokturk, E. Piskin, T. F. Serhatkulu, M. Cakmak, *Polym. Eng. Sci.* **2002**, *42*, 1619.
[17] L. Aliotta, P. Cinelli, M. B. Coltelli, M. C. Righetti, M. Gazzano, A. Lazzeri, *Eur. Polym. J.* **2017**, *93*, 822.
[18] K. Das, D. Ray, I. Banerjee, N. R. Bandyopadhyay, S. Sengupta, A. K. Mohanty, M. Misra, *J. Appl. Polym. Sci.* **2010**, *118*, 143.
[19] H. Bai, C. Huang, H. Xiu, Q. Zhang, H. Deng, K. Wang, F. Chen, Q. Fu, *Biomacromolecules* **2014**, *15*, 1507.
[20] W. Wang, A. Saperdi, A. Dodero, M. Castellano, A. J. Müller, X. Dong, D. Wang, D. Cavallo, *Cryst. Growth des.* **2021**, *21*, 5880.
[21] M. Brinkmann, S. Pratontep, C. Chaumont, J.-C. Wittmann, *Macromolecules* **2007**, *40*, 9420.
[22] C. Vergnat, V. Landais, J.-F. Legrand, M. Brinkmann, *Macromolecules* **2011**, *44*, 3817.
[23] Y. Li, R. Xin, S. Wang, Z. Guo, X. Sun, Z. Ren, H. Li, L. Li, S. Yan, *Macromolecules* **2021**, *54*, 9124.
[24] J. Petermann, J. M. Schultz, *Colloid Polym. Sci.* **1984**, *262*, 217.
[25] Y. J. Park, S. J. Kang, C. Park, B. Lotz, A. Thierry, K. J. Kim, J. Huh, *Macromolecules* **2008**, *41*, 109.
[26] W. A. Memon, R. Zhou, Y. Zhang, Y. Wang, L. Liu, C. Yang, J. Zhang, A. Liaqat, L. Xie, Z. Wei, *Adv. Funct. Mater.* **2022**, *32*, 2110080.
[27] J. Wang, Y. Liu, L. Hua, T. Wang, H. Dong, H. Li, X. Sun, Z. Ren, S. Yan, *ACS Appl. Polym. Mater* **2021**, *3*, 2098.
[28] J. C. Wittmann, P. Smith, *Nature* **1991**, *352*, 414.
[29] J.-F. Moulin, M. Brinkmann, A. Thierry, J.-C. Wittmann, *Adv. Mater.* **2002**, *14*, 436.
[30] M. Brosset, L. Herrmann, C. Kiefer, T. Falher and M. Brinkmann, submitted manuscript.
[31] K. Tremel, F. S. U. Fischer, N. Kayunkid, R. D. Pietro, R. Tkachov, A. Kiriy, D. Neher, S. Ludwigs, M. Brinkmann, *Adv. Energy Mater.* **2014**, *4*, 1301659.
[32] L. Biniek, S. Pouget, D. Djurado, E. Gonthier, K. Tremel, N. Kayunkid, E. Zaborova, N. Crespo-Monteiro, O. Boyron, N. Leclerc, S. Ludwigs, M. Brinkmann, *Macromolecules* **2014**, *47*, 3871.
[33] A. Hamidi-Sakr, L. Biniek, S. Fall, M. Brinkmann, *Adv. Funct. Mater.* **2016**, *26*, 408.
[34] H. Li, M. A. Huneault, *Polymer* **2007**, *48*, 6855.
[35] J. Muller, A. Jiménez, C. González-Martínez, A. Chiralt, *Polym. Int.* **2016**, *65*, 970.
[36] H. T. Oyama, S. Abe, *ACS Sustainable Chem. Eng.* **2015**, *3*, 3245.
[37] D. Sawai, M. Tamada, T. Kanamoto, *Polym. J.* **2007**, *39*, 953.
[38] M. Takasaki, H. Ito, T. Kikutani, *J. Macromol. Sci., Phys.* **2003**, *B42*, 403.

26424169, 0, Downloaded from https://onlinelibrary.wiley.com/doi/10.1002/pol.20220740 by Cochrane France, Wiley Online Library on [10/03/2023]. See the Terms and Conditions (https://onlinelibrary.wiley.com/terms-and-conditions) on Wiley Online Library for rules of use; OA articles are governed by the applicable Creative Commons License

[39] Z.-C. Zhang, X.-R. Gao, Z.-J. Hu, Z. Yan, J.-Z. Xu, L. Xu, G.-J. Zhong, Z.-M. Li, *Ind. Eng. Chem. Res.* **2016**, *55*, 10896.
[40] P. Pan, J. Yang, G. Shan, Y. Bao, Z. Weng, A. Cao, K. Yazawa, Y. Inoue, *Macromolecules* **2012**, *45*, 189.
[41] P. Pan, Y. Inoue, *Prog. Polym. Science* **2009**, *34*, 605.
[42] C. Vergnat, V. Landais, J. Combet, A. Vorobiev, O. Konovalov, J.-F. Legrand, M. Brinkmann, *Org. Electron.* **2012**, *13*, 1594.
[43] H. M. Schrickx, P. Sen, R. E. Booth, A. Altaqui, J. Burleson, J. J. Rech, J.-W. Lee, M. Biliroglu, K. Gundogdu, B. J. Kim, W. You, M. W. Kudenov, B. T. O'Connor, *Adv. Funct. Mater.* **2022**, *32*, 2105820.

SUPPORTING INFORMATION

Additional supporting information can be found online in the Supporting Information section at the end of this article.

How to cite this article: M. Brosset, L. Herrmann, T. Falher, M. Brinkmann, *J. Polym. Sci.* **2023**, 1. https://doi.org/10.1002/pol.20220740

26424169, 0, Downloaded from https://onlinelibrary.wiley.com/doi/10.1002/pol.20220740 by Cochrane France, Wiley Online Library on [10/03/2023]. See the Terms and Conditions (https://onlinelibrary.wiley.com/terms-and-conditions) on Wiley Online Library for rules of use; OA articles are governed by the applicable Creative Commons License